POLITECNICO
MILANO 1863

RE.PUBLIC@POLIMI
Research Publications at Politecnico di Milano

Post-Print

This is the accepted version of:

L. Keulen, S. Gallarini, C. Landolina, A. Spinelli, P. Iora, C. Invernizzi, L. Lietti, A. Guardone
Thermal Stability of Hexamethyldisiloxane and Octamethyltrisiloxane
Energy, Vol. 165, 2018, p. 868-876
doi:10.1016/j.energy.2018.08.057

The final publication is available at https://doi.org/10.1016/j.energy.2018.08.057

Access to the published version may require subscription.

When citing this work, cite the original published paper.

© 2018. This manuscript version is made available under the CC-BY-NC-ND 4.0 license
http://creativecommons.org/licenses/by-nc-nd/4.0/

Permanent link to this version
http://hdl.handle.net/11311/1072889

Thermal stability of hexamethyldisiloxane and octamethyltrisiloxane

L. Keulen[a], S. Gallarini[c], C. Landolina[b], A. Spinelli[c], P. Iora[d], C. Invernizzi[d], L. Lietti[c], A. Guardone[a,*]

[a]*Department of Aerospace Science & Technology, Politecnico di Milano, Via La Masa 34, 20156 Milano, Italy*
[b]*Department of Mechanical Engineering, Politecnico di Milano, Via La Masa 1, 20156 Milano, Italy*
[c]*Energy Department, Politecnico di Milano, Via Lambruschini 4, 20156 Milano, Italy*
[d]*Department of Mechanical and Industrial Engineering, University of Brescia, Via Branze 38, 25121 Brescia, Italy*

Abstract

A novel test-rig for studying the thermal stability of working fluids for ORC applications was designed and commissioned at the Laboratory of Compressible-fluid dynamics for Renewable Energy Applications (CREA Lab) of Politecnico di Milano, in collaboration with the University of Brescia. The set-up is composed by a vessel containing the fluid under scrutiny, heated for about 80 hours at a constant stress temperature. During the test, the pressure is monitored to detect thermal decomposition of the fluid. After the test, the vessel is placed in a thermal bath, where the vapor pressure is measured at different values of temperature lower than the stress temperature and critical temperature and is compared to that obtained before the fluid underwent thermal stress. If departure from the initial fluid behavior is observed, thermal decomposition occurred and a chemical analysis of the sample is carried

*Corresponding author.
Email address: alberto.guardone@polimi.it (A. Guardone)

out on both liquid and vapor phase using gas chromatography and mass spectrometry.

Experimental results are reported for the pure siloxane fluids MM (Hexamethyldisiloxane, $C_6H_{18}OSi_2$) and MDM (Octamethyltrisiloxane, $C_8H_{24}O_2Si_3$), showing that limited but appreciable decomposition is occurring at 240 °C and 260 °C respectively.

Keywords:

Thermal stability, Thermal decomposition, Organic Rankine cycle working fluids, MM, Hexamethyldisiloxane, MDM, Octamethyltrisiloxane, Linear siloxanes, Organic fluids, ORC applications

---

1. Introduction

Power cycles based on the Rankine cycle using water as working fluid are traditionally used in large power plants [1]. Due to the growing attention to energy efficiency and environmental issues, the organic Rankine cycle (ORC) is now a widely used technology for small to medium scale power generation. They are used for many different applications, from industrial waste heat recovery to renewable energy applications, such as solar, biomass and geothermal energy [2, 3, 4, 5] and in general whenever relatively low temperature energy sources are available [6, 7]. The key-difference of ORCs in comparison with traditional power cycles is the use of organic compounds as working fluids. ORCs are coupled to low/medium temperature heat sources (less than 500 °C) in small/medium power plants (up to 100 MW) [1, 8]. For these applications the use of fluids with high molecular mass and high molecular complexity is usually a better option with respect to water. The

advantage of using organic compounds lies in the design and construction of the power plants, which are simpler, more reliable, and cheaper than steam Rankine cycle plants for the small to medium power range and keep the same good cycle efficiency [8].

A key aspect of the design of an ORC power plant is the selection of the working fluid. It essentially depends on the source temperature and has a great influence on the components of the power plant, namely heat exchangers, expander, condenser, and pump.

The use of a working fluid is restricted by its thermal stability limit, namely the temperature beyond which the fluid undertakes a significant structural decomposition. This can have a large impact on the system and cause loss of power or serious malfunctions of fundamental components [9, 10]. Moderate decomposition gives rise to mixtures which might modify the physical and thermodynamic properties of the working fluid and influence cycle performance. However, if mixture properties are known, the system can be adapted reducing loss of power or without replacing the working fluid [11].

Pure siloxane working fluids are prominent, successful working fluids for ORCs. Thanks to their high thermal stability range, siloxanes are of interest for high temperature applications of ORCs [12]. Siloxane fluids can be separated into two groups, linear and cyclic polymers, and are composed of alternating silicon oxygen atoms with methyl groups attached to the silicon atoms [13]. In principle, these siloxanes can all be used as working fluids in ORCs depending on the power level and heat source temperature [14]. For the use of siloxanes, reliable data about thermal stability is necessary as highlighted by Colonna et al. [1]. Several effects can influence the stability

of the working fluid besides temperature, such as:

- the presence of impurities, especially water and oxygen, which are almost always present in an actual plant;
- the time span of stress at a given temperature, since stressing the fluid at low temperature for a long period of time can also cause degradation;
- the pressure.

Some literature data about thermal stability limits of pure siloxanes are available. Colonna et al. [15] report limits of 400 °C for siloxanes, Angelino and Invernizzi [16] provide similar results for cyclic siloxanes. An extensive research on polysiloxanes have been conducted by Dvornic [17] but without mentioning degradation temperatures. A recent study by Preißinger and Brüggemann [12] shows a thermal stability temperature of 300 °C for hexamethyldisiloxane (MM) and annual degradation rate of less than 3.5%. No literature can be found about the thermal stability of siloxane MDM.

The method used in this research was introduced by Blake et al. [18], who applied it to more than one hundred organic fluids from twelve different chemical families. This methodology is based on the analysis of isothermal pressure deviations of fluids subjected to different thermal stress temperatures. Later, Fisch and Verderame [19], Johns et al. [20, 21], and Fabuss et al. [22] used this method. Calderazzi and Colonna di Paliano [23] introduced the comparison of the vapor pressure before and after the thermal stress and the chemical analysis of the liquid fraction to determine if decomposition of the fluid occurred and applied it to refrigerants. This method has proven to be more effective in detecting even limited decomposition effects than analyzing

the pressure during the isothermal stress test. Later, Angelino and Invernizzi [24] applied this methodology to zero ODP refrigerants. Pasetti et al. [25] improved the data analysis method and applied it to organic Rankine cycle fluids.

This research focuses on the determination of the thermal stability limit and decomposition products of siloxane fluids hexamethyldisiloxane (MM) and octamethyltrisiloxane (MDM). The method and experimental apparatus in this research is based on the methodology of Calderazzi and Colonna di Paliano [23] and Pasetti et al. [25] and uses statistical analysis to determine decomposition based on the deviation in vapor pressure introduced in Pasetti et al. [25]. The experimental apparatus is based on the one proposed in Pasetti et al. [25], improved in order to allow the performance of chemical analysis on the decomposition products on both vapor and liquid phase.

The paper is structured as follows: the experimental apparatus is presented in Section 2, the measurement procedure and data analysis are reported in Sections 3 and 4 respectively. Tests results are reported and commented in Section 5, while conclusions are drawn in Section 6.

2. Experimental apparatus

The experimental apparatus is based on the design of Calderazzi and Colonna di Paliano [23] and Pasetti et al. [25]. The set-up was improved for measurements on siloxane fluids and chemical analysis of both liquid and vapor phase. Due to the low vapor pressures of siloxanes [26] at temperatures close to the ambient one, the apparatus is designed to measure low pressures down to 2 mbar. To have the ability of measuring a large range of

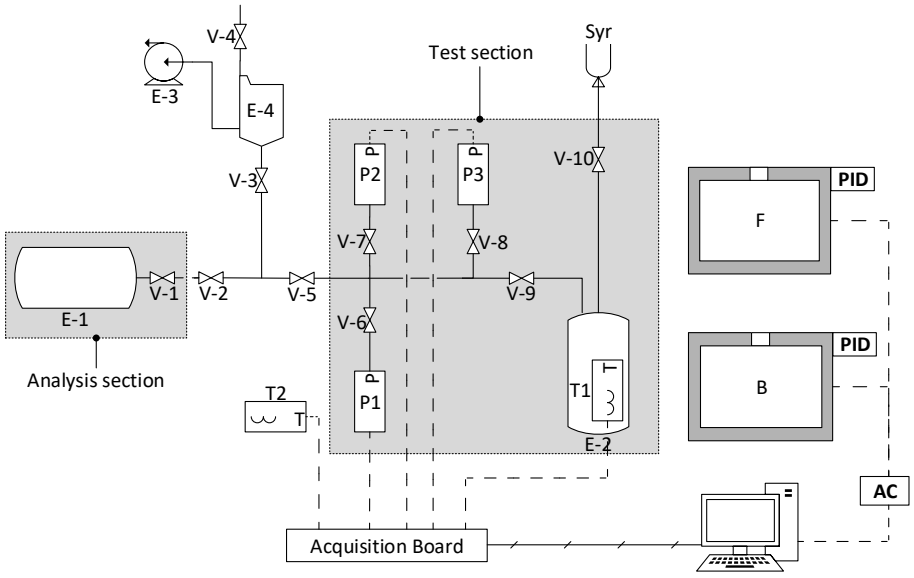

Figure 1: Schematic diagram of the experimental apparatus: temperature controlled oven (F), thermal bath (B), 150 cm^3 vessels (E-1,2), pressure transducers (P-1,2,3), thermocouples (T-1,2), valves (V), vacuum pump (E-3), vacuum trap (E-4), loading syringe (Syr)

pressures (related to the difference between stress temperatures and vapor pressure measurement temperatures) while having good accuracy during the vapor pressure measurement, the apparatus is equipped with three different pressure transducers with 1 bar, 10 bar, and 35 bar full scale. Two thermocouples of T and K type, are used to acquire the temperature during the vapor pressure measurement and during thermal stress respectively. Because of the goal of performing chemical analysis on both the liquid and vapor phase, a section is added for the vapor extraction. This is done to capture the more volatile products of thermal decomposition.

The schematic design of the apparatus used for the thermal stability measurement is shown in Fig. 1. It is divided into two sections, the test section, which is used for the vapor pressure measurement and thermal stress test, and the analysis section, which is used to collect the gas sample for chemical analysis. The liquid sample is taken from the test vessel, by disassembling it from the rest of the apparatus. The vacuum pump (E-3) is used to evacuate the test and analysis section. The fluid is loaded through a syringe (Syr) connected to the test section.

The thermal bath (B) is used for the measurement of the vapor pressure. The heat transfer oil has a temperature range of $-20\,^{\circ}\mathrm{C}$ to $200\,^{\circ}\mathrm{C}$. The temperature of the bath is controlled by a PID controller with a stability of $\pm 0.02\,^{\circ}\mathrm{C}$. The furnace (F) is used for the thermal stress test, and the temperature can be varied from $25\,^{\circ}\mathrm{C}$ to $1200\,^{\circ}\mathrm{C}$ with a stability of $\pm 2\,^{\circ}\mathrm{C}$ controlled by a PID controller.

The tubing, connectors, valves, and vessels in the test section are made from 316L stainless-steel. The vessels (E-1,2) have a volume of approximately $150\,\mathrm{cm}^3$. The sample vessel is connected by a TIG welding to three tubes for the housing of the thermocouple (thermowell), the loading of the system and the connection to the measuring section. The total inner volume of the circuit is approximately $230\,\mathrm{cm}^3$.

The measurement instrumentation includes three absolute capacitive pressure transducers (P-1,2,3) and two thermocouples (T-1,2). The pressure transducers have full scale of 1 bar, 10 bar, and 35 bar and expanded uncertainty of 0.6 mbar, 6 mbar, and 21 mbar respectively. Possible zero offset of the pressure readings are compensated at atmospheric conditions through

Table 1: Pressure transducer specifications.

Technology	Capacitance sensor
Measured quantity	Absolute Pressure
Full scale	1 bar, 10 bar, 35 bar
Expanded uncertainty	0.6 mbar, 6 mbar, 21 mbar

Table 2: Thermocouples specifications.

Type	T	K
Range	$-133\,^{\circ}\mathrm{C}$ to $400\,^{\circ}\mathrm{C}$	$-270\,^{\circ}\mathrm{C}$ to $1370\,^{\circ}\mathrm{C}$
Tolerance	$1\,^{\circ}\mathrm{C}$ for $T = [-133; 133]\ ^{\circ}\mathrm{C}$	$2.5\,^{\circ}\mathrm{C}$ for $T = [-270; 333]\ ^{\circ}\mathrm{C}$
	$0.0075T$ for other T	$0.0075T$ for other T

a comparison with pressure measured by a high accuracy barometer. The thermocouples are of T-type for the vapor pressure measurement phase and of K-type for the thermal stress phase, with expanded uncertainty of $1\,^{\circ}\mathrm{C}$ and $2.5\,^{\circ}\mathrm{C}$ respectively.

Chemical analysis are performed on the liquid and vapor sample separately. The liquid phase is analyzed by gas chromatography with two capillary columns coupled with a flame ionization detector and a mass spectrometer. The first permits the semi-quantitative reconstruction of the sample composition, while the latter allows the identification of the mixture components. Regarding the vapor phase, the arrangement is similar to the liquid one, except for the column, which is specific for light compounds, and the detector, that is of the thermal conductivity type.

In Table 1 and Table 2 are reported thermocouples and pressure trans-

ducers specifications.

3. Measurement procedure

The procedure used to determine the thermal stability and decomposition of the fluids is described in this section.

3.1. Preparation of test

To remove all impurities, the entire test section is disassembled and heated at 80 °C. Subsequently, the test section is reassembled and evacuated. The system is exposed to ambient air and the possible zero offset of pressure transducers is compensated by comparison with a reference barometer. Finally, the system is tested for leakages in vacuum and pressurized conditions.

The fluid quantity to be loaded into the circuit is determined considering that:

1. the pressure must not exceed the highest pressure transducer FS ($P_{FS} = 35\,\mathrm{bar}$) at maximum thermal stress temperature T_{stress};

2. during the vapor pressure measurement the fluid must remain in two-phase conditions;

3. the fluid must be in the vapor phase during the thermal stress tests.

The requirement that leads to a lower allowable mass sets the maximum mass that can be loaded.

The required fluid mass m of fluid is loaded into the test vessel by filling a syringe connected to the test section as shown in Fig. 1. Note that it is not relevant that the loaded fluid mass is controlled with high precision, since the

influence of m on test results is negligible once it is in the range determined by the three conditions set above.

After the loading procedure, the fluid is degassed to remove air and other non-condensible gases. The test vessel is heated using the thermal bath at 50 °C for one hour to facilitate the liquid phase gas expulsion. Subsequently the fluid is cooled down, maintained at −20 °C and degassed using the vacuum pump. This procedure is repeated until the pressure after two consecutive steps returns to the same value, to ensure that the largest amount of non-condensible gases is extracted from the system.

3.2. Thermal stability measurement

The core of the thermal stability test is presented here.

Vapor pressure measurement of the reference fluid

The vapor pressure of the non-stressed fluid, also called reference fluid, is measured as reference to determine decomposition by comparison with the stressed fluids vapor pressure over a range of temperature. The temperature interval is chosen taking into account the temperature range of the thermal bath and the accuracy of the lowest full scale pressure transducer so the pressure remains above the transducers uncertainty during the vapor pressure measurement. Each pair of $P-T$ values, obtained for n different thermal bath set-point temperature T, is recorded for 10 min and data are then averaged to obtain n different $P_i - T_i$ $(i = 1 \dots n)$ vapor pressure points.

Thermal stress test

The sample vessel containing the fluid under scrutiny is placed in the furnace for 80 h at a constant temperature T_{stress}. During the test, pressure

and temperature are monitored by the acquisition system.

Vapor pressure measurement of the stressed fluid

After the thermal stress test, the vapor pressure of the stressed fluid is measured using the same experimental procedure and temperature range as for the reference fluid.

3.3. Fluid extraction and chemical analysis

Chemical analysis is performed after the vapor pressure curve measurement relative to the highest temperature thermal stress. Both liquid and vapor phase of the stressed fluid are evaluated.

To extract the vapor phase, the system is pressurized (ca. 2 bar) with a He/N_2 /Ar mixture to dilute the gases formed upon decomposition of the fluid, if any, and to permit the feeding of the gas chromatograph. The analysis vessel (E-1) is eventually detached from the apparatus and the gaseous mixture is analyzed by gas chromatography and mass spectrometry. This method allows the quali-quantitative analysis of the gaseous species formed upon the thermal treatment of the fluid.

The composition of the liquid fraction of the stressed fluid is also determined; for this purpose liquid samples are taken and analyzed by gas chromatography and mass spectrometry. This allows the determination of compounds present in the liquid phase and their concentration.

4. Data analysis

To evaluate the thermal stability and decomposition of the stressed fluid, three analysis are conducted. They consist in the measurement of:

1. deviations of pressure at constant temperature during each thermal stress test;

2. deviations of fluid vapor pressure from reference fluid vapor pressure, after it underwent each thermal stress test;

3. compositions of the decomposed fluid.

The analysis of the pressure deviation during the thermal stress tests is an adequate method to detect large decomposition phenomena, but it is inadequate to identify weaker ones. Vapor pressure deviations are thus evaluated at low temperature because the influence of volatile compounds (typically formed upon decomposition) on saturated fluid $P - T$ curve is much more appreciable. This method allows a more sensitive evaluation of decomposition phenomena. Chemical analysis of the liquid and gas phase are finally performed (only after the highest stress temperature test) to identify the decomposition products and their quantity.

4.1. Pressure deviation during thermal stress test

The first evaluation is the analysis of the pressure deviation during the thermal stress tests. Because of the difficulty in reproducing and maintaining exact isothermal conditions during the thermal stress, the analysis is performed by comparing the percentage deviation of pressure and temperature over time. Any deviation in pressure that is not supported by a comparable deviation in temperature indicates possible thermal decomposition, but if no variation is observed it is not possible to claim that no decomposition occurred.

4.2. Deviation of vapor pressure from reference

The second evaluation is based on the deviation of the stressed fluids vapor pressure from the reference fluid vapor pressure, as described by Pasetti et al. [25]. The purpose of the vapor pressure analysis is the identification of deviations that can not be justified by measurement uncertainties. The vapor pressure of the virgin fluid and of the stressed fluid after each stress test are measured (see Section 3) and compared. Any deviation in vapor pressure indicates a change in composition, thus thermal decomposition.

First, the vapor pressure curve of the non-stressed fluid is evaluated. The vapor pressure data of the reference fluid are fitted with the Clausius-Clapeyron equation [27]

$$\frac{dP_{\mathrm{vap}}}{dT} = \frac{\Delta h_{\mathrm{v}}}{T\Delta v_{\mathrm{v}}} = \frac{\Delta h_{\mathrm{v}}}{(RT^2/P_{\mathrm{vap}})\Delta Z_{\mathrm{v}}}, \tag{1}$$

that can be rearranged to obtain

$$\frac{d\ln(P_{\mathrm{vap}})}{d(1/T)} = -\frac{\Delta h_{\mathrm{v}}}{R\Delta Z_{\mathrm{v}}}, \tag{2}$$

where P_{vap} is the saturated vapor pressure, T the temperature, Δh_{v} the specific enthalpy of vaporization, Δv_{v} the difference in specific volume between saturated liquid and saturated vapor, ΔZ_{v} the differences in compressibility factor between saturated liquid and saturated vapor, and R the specific gas constant. The ratio $\Delta h_{\mathrm{v}}/\Delta Z_{\mathrm{v}}$ is nearly independent of temperature in a wide thermodynamic region [27], so Eq. (2) can be integrated obtaining

$$P_{\mathrm{vap}} = \exp\left(A - \frac{B}{T}\right), \tag{3}$$

where A is the integration constant and $B = \Delta h_{\mathrm{v}}/(R\Delta Z_{\mathrm{v}})$.

The vapor pressure data of the reference fluid are fitted with Eq. (3) to obtain an equation for the reference pressure as function of temperature:

$$P_{\mathrm{ref}}(T) = \exp\left(A - \frac{B}{T}\right). \tag{4}$$

Due to the assumption of negligible variation of the ratio $\Delta h_{\mathrm{v}}/\Delta Z_{\mathrm{v}}$ with temperature, Eq. (4) is a good approximation for vapor pressure only over small temperature intervals, as are those of interest here.

The total number of vapor pressure data points n are interpolated obtaining the reference vapor pressure curve. Two new variables

$$x_i = \frac{1}{T_i}, \qquad i = 1 \ldots n \tag{5a}$$

$$y_i = \ln(P_i) \qquad i = 1 \ldots n \tag{5b}$$

are introduced to perform standard linear regression and obtain coefficients A and B.

The uncertainty of the reference equation is given by

$$u^2\left(P_{\mathrm{ref}}\right) = u^2_{\mathrm{mod}}(P_{\mathrm{ref}}) + u^2_{\mathrm{ins}}(P_{\mathrm{ref}}) \tag{6}$$

which is the sum of the uncertainties related to the model $u^2_{\mathrm{mod}}(P_{\mathrm{ref}}(T))$ and uncertainty contribution of the measurement instruments $u^2_{\mathrm{ins}}(P_{\mathrm{ref}}(T))$ [25].

The uncertainty contributed by the instruments is obtained propagating measurement uncertainties through the reference vapor pressure equation, leading to

$$u^2_{\mathrm{ins}}(P_{\mathrm{ref}}) = \left[\frac{\partial P_{\mathrm{ref}}}{\partial T} u_{\mathrm{ins}}(T)\right]^2 + u^2_{\mathrm{ins}}(P), \tag{7}$$

where $u_{\mathrm{ins}}(T)$ is the thermocouple uncertainty and $u_{\mathrm{ins}}(P)$ the pressure transducer uncertainty (see Table 1 and Table 2).

Subsequently the deviation is determined at temperature T, between the vapor pressure of the fluid after the thermal stress test $P_{T_{\text{stress}}}|_T$ and the reference fluid $P_{\text{ref}}(T)$, which is defined as

$$\Delta P^{\text{ref}}_{T_{\text{stress}}}|_T = P_{T_{\text{stress}}}|_T - P_{\text{ref}}(T)|_T. \tag{8}$$

The temperature at which the stressed fluid vapor pressure is measured is used to calculate the reference pressure $P_{\text{ref}}(T)$ using Eq. (4). The uncertainty of the deviation is expressed taking in account the uncertainty contribution of the measuring instruments and of the reference vapour pressure curve as

$$u^2\left[\Delta P^{\text{ref}}_{T_{\text{stress}}}|_T\right] = u^2(P_{T_{\text{stress}}}|_T) + u^2(P_{\text{ref}}|_T) \tag{9}$$

where the uncertainty of the stressed fluid vapor pressure measurement is defined as

$$u^2\left(P_{T_{\text{stress}}}|_T\right) = u^2_P(P), \tag{10}$$

with $u^2_P(P)$ being a combination of the measuring instrument uncertainties and the contribution of variance of the measured temperature and pressure data points for a fixed thermal bath set-point temperature.

To assess if the difference in vapor pressure is statistically significant (i.e. if it is attributable to decomposition and not to measurement uncertainties), $\Delta P^{ref}_{T_{\text{stress}}}|_T$ must be compared to $u\left(\Delta P^{\text{ref}}_{T_{\text{stress}}}|_T\right)$. This comparison can be carried out considering, as suggested by Pasetti et al. [25], the confidence index of the vapor pressure deviation $i_C(\Delta P^{ref}_{T_{\text{stress}}}|_T)$, defined as

$$i_C(\Delta P^{\text{ref}}_{T_{\text{stress}}}|_T) = \frac{\Delta P^{\text{ref}}_{T_{\text{stress}}}|_T}{u\left(\Delta P^{\text{ref}}_{T_{\text{stress}}}|_T\right)}. \tag{11}$$

The confidence index is equal to the coverage factor to be applied to justify the deviation of $\Delta P^{\text{ref}}_{T_{\text{stress}}}|_T$ from zero with measurement uncertainties. From

this it follows that the larger the confidence index, the lower is the probability that the deviation from the reference value can be justified by the measurement uncertainty. The confidence level values of $p_1 = 90\%$ and $p_2 = 99\%$ with corresponding coverage factors of $k_{p_1} = 1.645$ and $k_{p_2} = 2.576$ are taken as discriminant for three different cases:

- $|i_C(\Delta P)| \leq k_{p_1}$, the pressure deviation can be reasonably explained by the measurement uncertainty;
- $k_{p_1} < |i_C(\Delta P)| \leq k_{p_2}$, the pressure deviation can be explained by the measurement uncertainty only by extending it to high confidence levels, so the measured pressure change can be attributed, with high probability, to decomposition of the fluid;
- $|i_C(\Delta P)| > k_{p_2}$: the pressure deviation can be explained by extending the measurement uncertainty over the 99% confidence levels, so the pressure deviation certainly represents the effect of decomposition of the fluid.

5. Results and discussion

The test-rig is built to determine the thermal stability and decomposition products of working fluids for ORC applications. The thermal stability temperature of linear siloxane MM and MDM are determined and results are elaborated in the following sections. The fluids used are obtained from commercial sources and used without further purification.

5.1. Hexamethyldisiloxane (MM)

The fluid purity of MM before the stress tests as stated by the supplier is larger than 99.4%, which is confirmed by chemical analysis conducted on the fluid, listed in Table 3.

The sample of MM is tested for several temperatures following the procedure described in Section 3. The loaded MM sample has a mass of approximately 18 g and is stressed from 200 °C to 340 °C with increments of $\Delta T = 20\,°\mathrm{C}$.

The vapor pressure is measured in the range between $-20\,°\mathrm{C}$ and $10\,°\mathrm{C}$, with increments of $\Delta T = 5\,°\mathrm{C}$. The measured vapor pressure data of the reference fluid P_{vap}, with 95% confidence uncertainty bars, along with the calculated reference curve P_{ref} are shown in Fig. 2.

The temperature and pressure are registered during the thermal stress test. During the tests no appreciable pressure deviations occur, which are not related to temperature fluctuations, thus showing no evidence of fluid decomposition, though relatively large temperature fluctuations are observed (up to 5%). This can be related to ambient temperature fluctuations in the room and cooled down fluid vapor returning from the measurement section outside of the oven into the sample vessel.

Although the analysis during the thermal stress test does not reveal thermal decomposition, the vapor pressure in Fig. 3 shows deviation from the reference fluid, thus indicating thermal decomposition. The confidence index analysis in Fig. 4 reveals that the 240 °C test is well above the 99% level of confidence, which represents with very high probability the effect of thermal decomposition. From 240 °C and higher the confidence index increases,

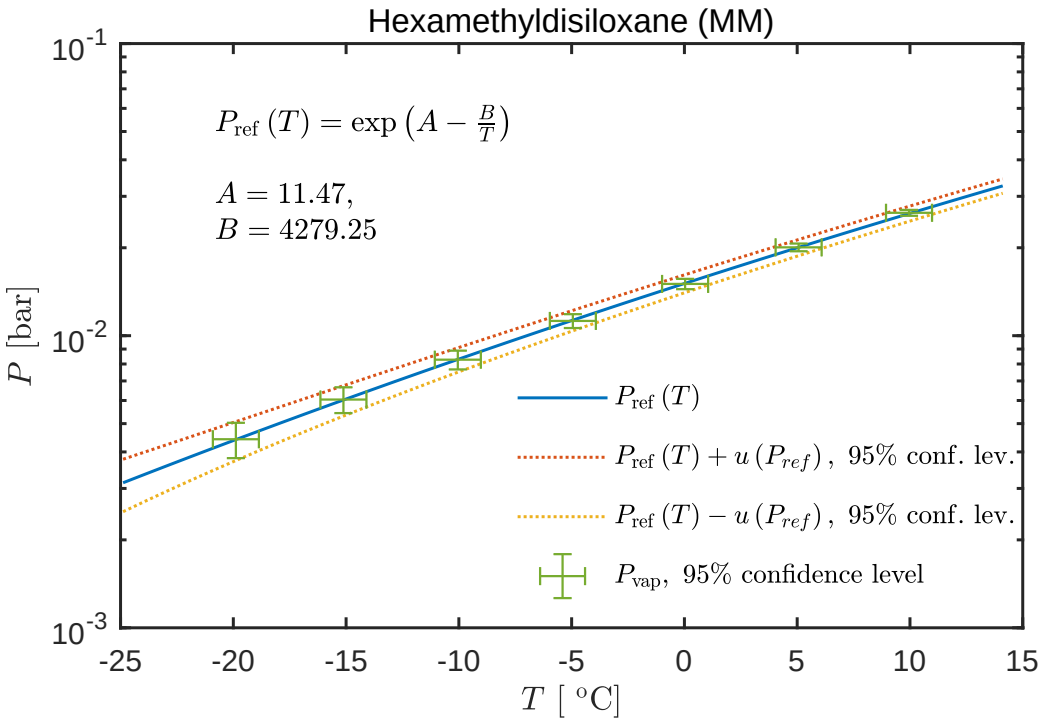

Figure 2: Vapor pressure of reference MM fluid. The figure shows the measured vapor pressure of the reference fluid (green bars) including 95% confidence level uncertainties. The reference curve is given by the blue line and the dotted lines show the upper and lower 95% confidence level uncertainty of the reference pressure curve.

indicating further decomposition.

Decomposition is also observed by chemical analysis, though it is very limited. Table 3 shows the composition of the reference liquid MM and of the stressed liquid phase, in relative percentage. The content of MM in the liquid phase decreases from 99.748% to 99.067%. Some components could not be verified by the used chemical species database and are listed as undefined. The vapor phase analysis in Table 4 shows that volatile gases in the order of µmol over a loaded amount of about 100 mmol are formed due

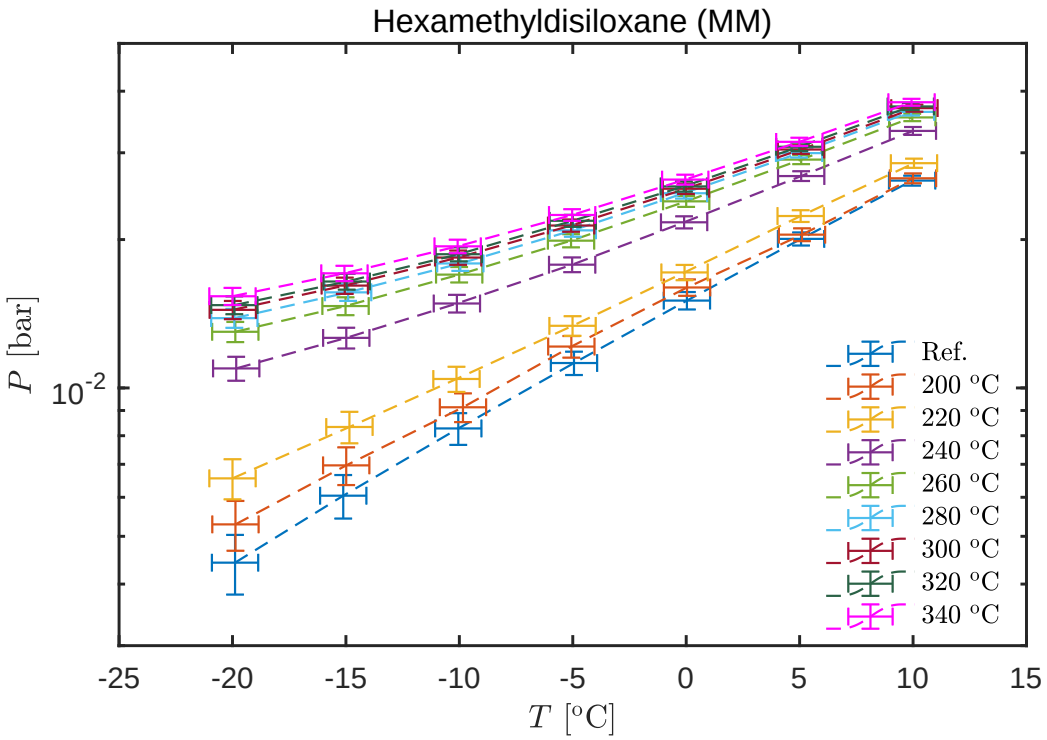

Figure 3: Vapor pressure measurement of MM after the different stress tests including 95% confidence level uncertainties.

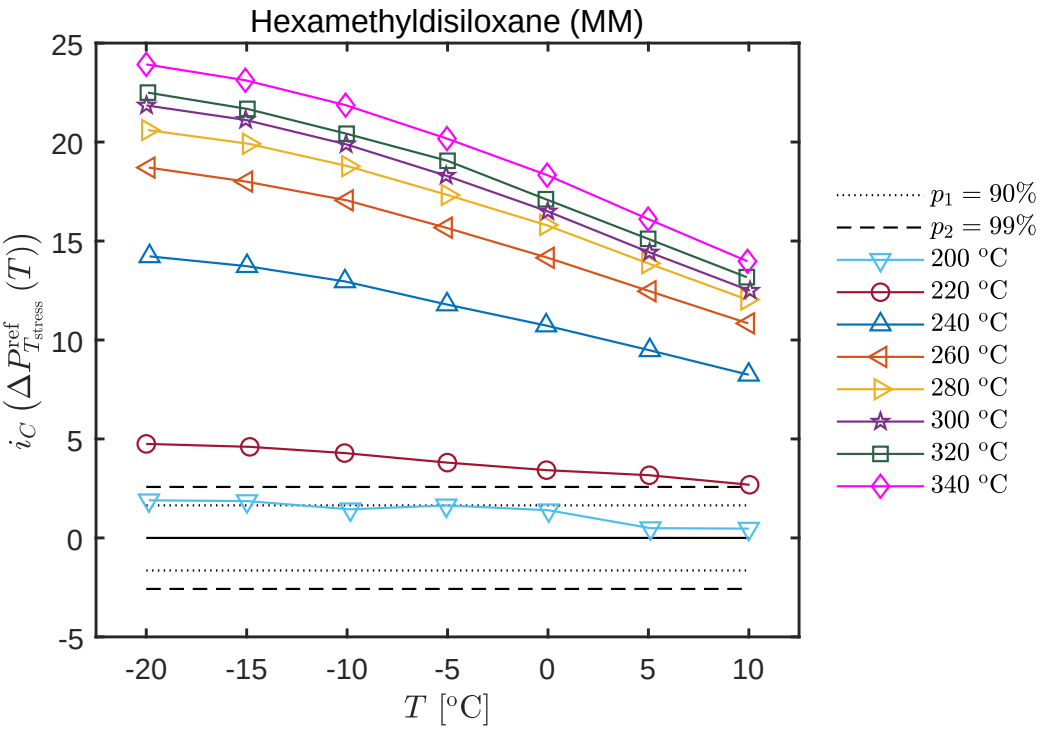

Figure 4: Confidence index of the vapor pressure deviation between the reference fluid and stressed MM fluid. The dashed lines $(--)$ represent the 99% confidence level and the dotted lines $(\cdots)$ the 90% confidence level.

Table 3: Chemical analysis results of liquid reference MM fluid and liquid phase of stressed MM fluid after 340 °C. The results for the reference fluid and liquid phase are given in relative percentage between detected components.

Component	Reference liquid [%]	Stressed liquid phase [%]
MOH	0.089	0.090
MM	99.748	99.067
D_3	-	0.015
D_4	0.002	0.683
Undefined	0.161	0.145

to decomposition.

To the author's knowledge, Preißinger and Brüggemann [12] is the only study about thermal stability of siloxane MM available in open literature so far. Decomposition products found in the vapor phase in the present work (see Table 4) are compatible with those reported in Preißinger and Brüggemann [12]. However, quantitative results of the present work are not directly comparable to those by Preißinger and Brüggemann [12]. Indeed, in this work chemical analysis were performed only once, after the thermal stress at 340 °C and on a sample that was previously stressed at 200 °C, 220 °C, 240 °C, 260 °C, 280 °C, 300 °C, 320 °C. Preißinger and Brüggemann [12] did not perform chemical analysis relative to thermal stress at 340 °C.

5.2. Octamethyltrisiloxane (MDM)

The fluid purity of MDM before the stress test as stated by the supplier is larger than 99.7%, which is confirmed by chemical analysis conducted on the reference fluid listed in Table 5.

Table 4: Chemical analysis results of vapor phase of stressed MM fluid given in µmol.

Component	Vapor [µmol]
Methane	1.19
Ethylene	0.057
Ethane	0.085
CO_2	0.256

Two samples of MDM were tested for several temperatures. The first sample (26 g) was stressed at 200 °C and 250 °C. Due to oven temperature control problems, this sample was compromised by a sudden increase of temperature and a new sample was loaded for further tests. The second sample of 18 g was stressed from 260 °C to 350 °C.

The vapor pressure is measured in the range between 10 °C and 50 °C, with increments of $\Delta T = 10\,°C$ from 10 °C to 30 °C and $\Delta T = 5\,°C$ from 30 °C to 50 °C. The measured vapor pressure data of the reference fluid P_{vap}, with 95% confidence level uncertainties, along with the calculated reference curve P_{ref} is shown in Fig. 5.

The temperature and pressure are registered during the thermal stress test. During the tests no pressure deviations occur, which are not related to temperature fluctuations, thus showing no evidence of fluid decomposition.

Although the analysis during the thermal stress test does not reveal thermal decomposition, the vapor pressure in Fig. 6 show deviation from the reference fluid, thus indicating thermal decomposition. The confidence index analysis in Fig. 7 reveals that, for $T_{\mathrm{stress}} = 260\,°C$, $\Delta P^{\mathrm{ref}}_{T_{\mathrm{stress}}}(T) \neq 0$ with high probability. This is an index of thermal decomposition. For stress tem-

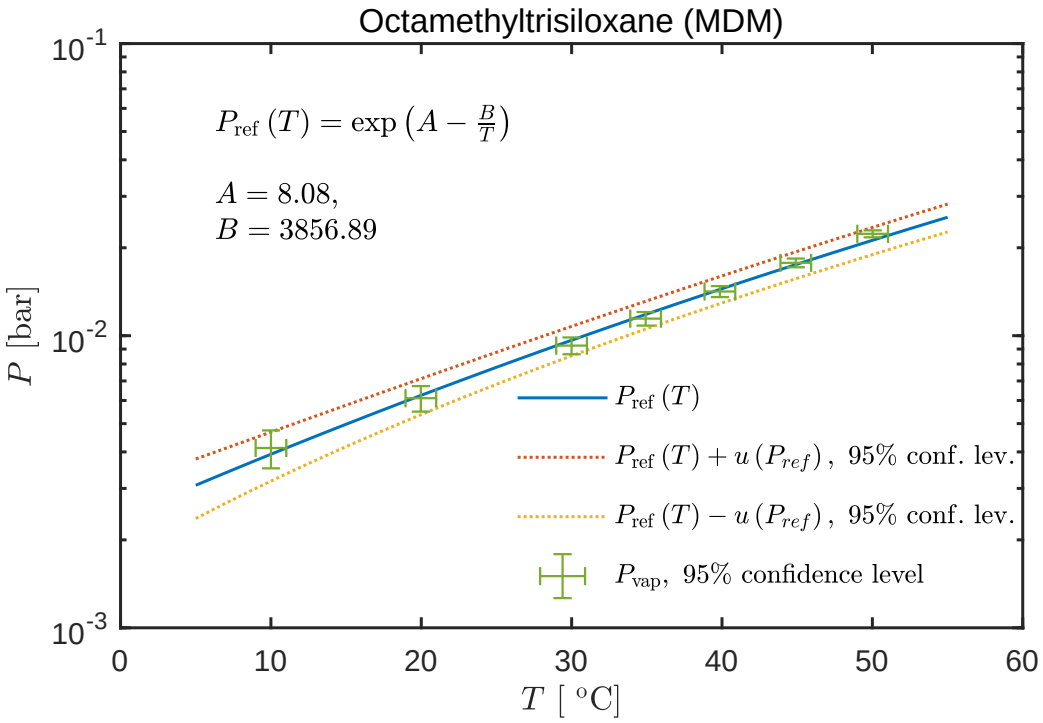

Figure 5: Vapor pressure of reference MDM fluid. The figure shows the measured vapor pressure of the reference fluid (green bars) including 95% confidence level uncertainties. The reference curve is given by the blue line and the dotted lines show the upper and lower 95% confidence level limit of the reference pressure curve.

peratures higher than 270 °C, the confidence index stagnates, indicating no significant change in vapor pressure. This could be related to the formation of heavy decomposition products, that can balance the increase of vapor pressure due to the formation of volatile compounds.

For MDM, limited decomposition is also observed by chemical analysis. Table 5 shows the composition of the reference liquid MDM and the stressed liquid phase. The MDM content in the liquid phase decreases from 99.972% to 99.917%. The vapor phase analysis shows that volatile gases are also

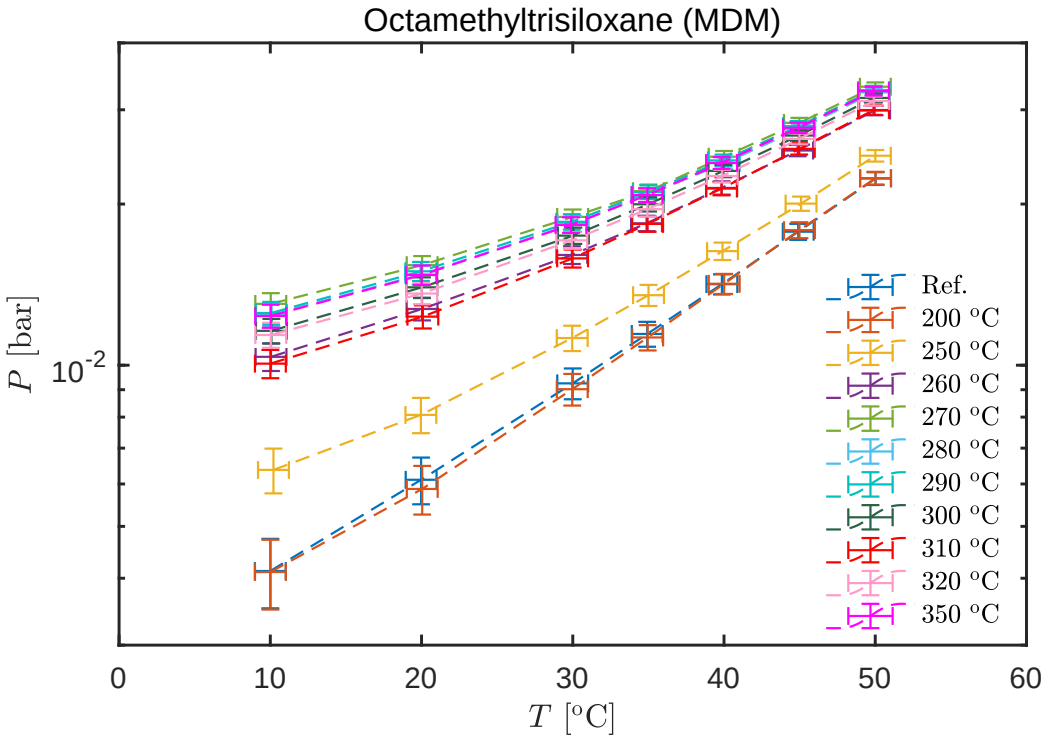

Figure 6: Vapor pressure measurement of MDM after the different stress tests including 95% confidence level uncertainties.

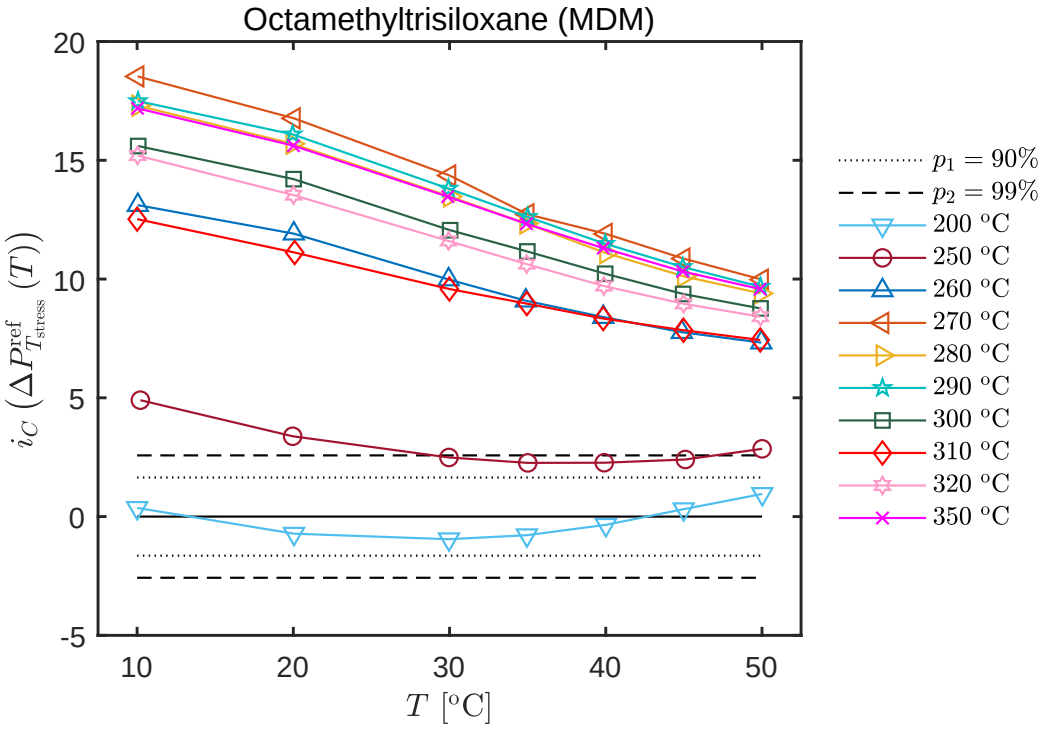

Figure 7: Confidence index of the vapor pressure deviation between the reference fluid and stressed MDM fluid. The dashed lines $(--)$ represent the 99% confidence level and the dotted lines $(\cdots)$ the 90% confidence level.

Table 5: Chemical analysis results of liquid reference MDM fluid and liquid phase of stressed MDM fluid. The results are given in relative percentage between detected components.

Component	Reference liquid [%]	Stressed liquid phase [%]
MOH	0.003	0.006
MM	0.003	0.018
MDM	99.972	99.917
D_4	0.012	0.014
MD_2M	0.004	0.011
Undefined	0.006	0.034

Table 6: Chemical analysis results of vapor phase of stressed MDM fluid given in µmol.

Component	Vapor [µmol]
Methane	0.948
Ethylene	0.025
Ethane	0.05
CO_2	0.524

formed for MDM in the order of µmol due to decomposition (see Table 6), while a quantity of the order of 100 mmol of pure MDM were loaded.

6. Conclusion

In this work the design of an experimental test-rig for the determination of thermal stability and decomposition products for ORC working fluids has been presented. The test-rig is designed to determine thermal stability tem-

peratures based on methods already used in literature, though the novelty introduced is the possibility to perform chemical analysis of the liquid and vapor phase. This is an important addition to fully determine the decomposition products.

Together with the description of the apparatus and test methodology, the thermal stability temperature and decomposition products of MM and MDM are assessed. MM is stressed under various temperatures ranging from 200 °C to 340 °C, while MDM is stressed between 200 °C and 350 °C. Both fluids were analyzed in terms of pressure deviation during the stress test as well as vapor pressure deviations from the reference fluid. Finally, chemical analysis were performed to determine the decomposition products, in both the liquid and the vapor phase. Pressure deviations during the thermal stress test show no sign of thermal decomposition.

Based on the results of the deviation of the vapor pressure from the reference fluid it can be seen that appreciable decomposition of MM occurs above 240 °C. Decomposition is also verified by chemical analysis of the liquid and vapor phase of the stressed fluid, though the decomposition is very limited. Volatile gases are formed as decomposition products; they can have a large impact on the fluid behavior because of their high vapor pressure, if compared to MM.

Analysis of the deviation of the vapor pressure from the reference fluid show that appreciable decomposition of MDM is occurring at 260 °C. Above 270 °C the decomposition rate appears to reduce. Though rearranging of molecules could occur, creating equilibrium conditions with varying compositions. Decomposition is also verified by chemical analysis of the liquid and

vapor phase of the stressed fluid, though the decomposition is very limited. Volatile gases are also formed as decomposition products from MDM.

It must be remarked that the results being presented here represent the temperature at which a change in composition can be detected by comparing vapor pressures at low temperature before and after a thermal stress carried out in an almost inert ambient (i.e. in a stailess steel container and without air, water or other pollutant). Thus the thermal stability limit in an industrial plant can be very different, due to the presence other chemical species.

References

[1] P. Colonna, E. Casati, C. Trapp, T. Mathijssen, J. Larjola, T. Turunen-Saaresti, A. Uusitalo, Organic Rankine Cycle Power Systems: From the Concept to Current Technology, Applications, and an Outlook to the Future, J. Eng. Gas Turbines Power 137 (10), URL http://dx.doi.org/10.1115/1.4029884.

[2] M. Wang, J. Wang, Y. Zhao, P. Zhao, Y. Dai, Thermodynamic analysis and optimization of a solar-driven regenerative organic Rankine cycle (ORC) based on flat-plate solar collectors, Appl. Therm. Eng. 50 (1) (2013) 816–825, URL http://dx.doi.org/10.1016/j.applthermaleng.2012.08.013.

[3] D. Meinel, C. Wieland, H. Spliethoff, Effect and comparison of different working fluids on a two-stage organic rankine cycle (ORC) concept,

Appl. Therm. Eng. 63 (1) (2014) 246–253, URL http://dx.doi.org/10.1016/j.applthermaleng.2013.11.016.

[4] A. Franco, Power production from a moderate temperature geothermal resource with regenerative Organic Rankine Cycles, Energy for Sustainable Development 15 (4) (2011) 411–419, URL http://dx.doi.org/10.1016/j.esd.2011.06.002.

[5] V. Minea, Power generation with {ORC} machines using low-grade waste heat or renewable energy, Appl. Therm. Eng. 69 (1-2) (2014) 143–154, URL http://dx.doi.org/10.1016/j.applthermaleng.2014.04.054.

[6] C. Invernizzi, P. Iora, Heat recovery from a micro-gas turbine by vapour jet refrigeration systems, Appl. Therm. Eng. 25 (8–9) (2005) 1233 – 1246, URL http://dx.doi.org/10.1016/j.applthermaleng.2004.08.008.

[7] C. Invernizzi, P. Iora, P. Silva, Bottoming micro-Rankine cycles for micro-gas turbines, Appl. Therm. Eng. 27 (1) (2007) 100 – 110, URL http://dx.doi.org/10.1016/j.applthermaleng.2006.05.003.

[8] E. Macchi, M. Astolfi, Organic Rankine Cycle (ORC) Power Systems. Technologies and applications, Woodhead Publishing Series in Energy: Number 107, Elsevier, New York, 2017.

[9] O. Badr, S. Probert, P. O'Callaghan, Selecting a working fluid for a Rankine-cycle engine, Appl. Energy 21 (1) (1985) 1–42, URL http://dx.doi.org/10.1016/0306-2619(85)90072-8.

[10] D. M. Ginosar, L. M. Petkovic, D. P. Guillen, Thermal Stability of Cyclopentane as an Organic Rankine Cycle Working Fluid, Energy & Fuels 25 (9) (2011) 4138–4144, URL http://dx.doi.org/10.1021/ef200639r.

[11] C. Invernizzi, D. Bonalumi, 5 - Thermal stability of organic fluids for Organic Rankine Cycle systems, in: E. Macchi, M. Astolfi (Eds.), Organic Rankine Cycle (ORC) Power Systems, Woodhead Publishing, ISBN 978-0-08-100510-1, 121 – 151, URL http://dx.doi.org/10.1016/B978-0-08-100510-1.00005-3, 2017.

[12] M. Preißinger, D. Brüggemann, Thermal Stability of Hexamethyldisiloxane (MM) for High-Temperature Organic Rankine Cycle (ORC), Energies 9 (3), URL http://dx.doi.org/10.3390/en9030183.

[13] F. Fernández, M. Prieto, I. Suárez, Thermodynamic analysis of high-temperature regenerative organic Rankine cycles using siloxanes as working fluids, Energy 36 (8) (2011) 5239 – 5249, URL http://dx.doi.org/10.1016/j.energy.2011.06.028.

[14] P. Colonna, A. Guardone, N. R. Nannan, Siloxanes: A new class of candidate Bethe-Zel'dovich-Thompson fluids, Phys. Fluids 19 (8) (2007) 086102, URL http://dx.doi.org/10.1063/1.2759533.

[15] P. Colonna, N. Nannan, A. Guardone, E. Lemmon, Multiparameter equations of state for selected siloxanes, Fluid Phase Equilib. 244 (2) (2006) 193 – 211, URL http://dx.doi.org/10.1016/j.fluid.2006.04.015.

[16] G. Angelino, C. Invernizzi, Cyclic Methylsiloxanes as Working Fluids for Space Power Cycles, J. Sol. Energy Eng. 115 (3), URL http://dx.doi.org/10.1115/1.2930039.

[17] P. R. Dvornic, Thermal Properties of Polysiloxanes, Springer Netherlands, Dordrecht, ISBN 978-94-011-3939-7, URL http://dx.doi.org/10.1007/978-94-011-3939-7_7, 2000.

[18] E. Blake, W. Hammann, J. W. Edwards, T. Reichard, M. R. Ort, Thermal Stability as a Function of Chemical Structure, J. Chem. Eng. Data 6 (1) (1961) 87–98, URL http://dx.doi.org/10.1021/je60009a020.

[19] K. R. Fisch, F. D. Verderame, Automatic Recording Apparatus for Thermal Stability Determinations, J. Chem. Eng. Data 6 (1) (1961) 131–134, URL http://dx.doi.org/10.1021/je60009a027.

[20] I. B. Johns, E. A. McElhill, J. O. Smith, Thermal Stability of Organic Compounds, I&EC Product Research and Development 1 (1) (1962) 2–6, URL http://dx.doi.org/10.1021/i360001a001.

[21] I. B. Johns, E. A. McElhill, J. O. Smith, Thermal Stability of Some Organic Compounds, J. Chem. Eng. Data 7 (2) (1962) 277–281, URL http://dx.doi.org/10.1021/je60013a036.

[22] M. A. Fabuss, A. S. Borsanyi, B. M. Fabuss, J. O. Smith, Thermal Stability Studies of Pure Hydrocarbons in a High Pressure Isoteniscope, J. Chem. Eng. Data 8 (1) (1963) 64–69, URL http://dx.doi.org/10.1021/je60016a018.

[23] L. Calderazzi, P. Colonna di Paliano, Thermal stability of R-134a, R-141b, R-13I1, R-7146, R-125 associated with stainless steel as a containing material, Int. J. Refrig 20 (6) (1997) 381 – 389, URL http://dx.doi.org/10.1016/S0140-7007(97)00043-1.

[24] G. Angelino, C. Invernizzi, Experimental investigation on the thermal stability of some new zero ODP refrigerants, International Journal of Refrigeration 26 (1) (2003) 51 – 58, ISSN 0140-7007, URL https://doi.org/10.1016/S0140-7007(02)00023-3, URL http://www.sciencedirect.com/science/article/pii/S0140700702000233.

[25] M. Pasetti, C. M. Invernizzi, P. Iora, Thermal stability of working fluids for organic Rankine cycles: An improved survey method and experimental results for cyclopentane, isopentane and n-butane, Appl. Therm. Eng. 73 (1) (2014) 764 – 774, URL http://dx.doi.org/10.1016/j.applthermaleng.2014.08.017.

[26] E. W. Lemmon, I. H. Bell, M. L. Huber, M. O. McLinden, NIST Standard Reference Database 23: Reference Fluid Thermodynamic and Transport Properties-REFPROP, Version 9.4.4.10, 2017.

[27] B. E. Poling, J. M. Prausnitz, J. P. O'Connell, The properties of gases and liquids, McGraw-Hill, New York, 5 edn., ISBN 0070116822 9780070116825, 2000.